QUARTERLY OF APPLIED MATHEMATICS
VOLUME LXXIII, NUMBER 4
DECEMBER 2015, PAGES 661–678
http://dx.doi.org/10.1090/qam/1397
Article electronically published on September 11, 2015

THE FUNDAMENTAL SOLUTION OF A CONSERVATION LAW WITHOUT CONVEXITY

By

YOUNGSOO HA (*Department of Mathematical Sciences, Seoul National University, Gwanakro 1, Gwanak-Gu, Seoul 151-747, Republic of Korea*)

AND

YONG-JUNG KIM (*National Institute of Mathematical Sciences, Daejeon 305-811, Republic of Korea, and Department of Mathematical Sciences, KAIST, Daejeon 305-701, Republic of Korea*)

Abstract. The nonnegative fundamental solution of a scalar conservation law is constructed when its flux may have a finite number of inflection points. The constructed solution can be either explicit and implicit depending on the flux. This fundamental solution consists of a series of rarefaction waves, contact discontinuities and a shock. These analytically constructed fundamental solutions are also compared with numerical approximations, which possess the structure of the analytically constructed fundamental solution.

Contents

1. Introduction 662
2. Preliminaries 663
3. Convex and concave envelopes 665
3.1. Convex envelope 665
3.2. Concave envelope 668
4. Construction of a fundamental solution 669
4.1. Nonconvex flux 669
4.2. Examples and comparison with a convex case 673
5. Numerical examples 675
References 677

Received January 19, 2014.
2000 *Mathematics Subject Classification.* Primary 35L67, 35L65, 76L05.
This work was supported by the National Institute of Mathematical Sciences and the National Research Foundation of Korea (NRF-2014M1A7A1A03029872).
E-mail address: youngamath.ha@gmail.com
E-mail address: yongkim@kaist.edu

©2015 Brown University

1. Introduction. The purpose of this paper is to construct the signed fundamental solution of a scalar conservation law,

$$\partial_t u + \partial_x f(u) = 0, \quad u(x,0) = u^0(x) \geq 0, \quad x \in \boldsymbol{R},\ t > 0, \tag{1.1}$$

explicitly or implicitly. A solution of (1.1) is called the fundamental solution of mass $m > 0$, denoted by $\rho_m(x,t)$ in this paper, if the initial value is the Dirac mass of the size given at the origin, i.e., if

$$\lim_{t\to 0} \rho_m(x,t) = m\delta(x). \tag{1.2}$$

We consider a nonconvex flux f under two hypotheses:

$$\begin{gathered} f \textit{ has a finite number of inflection points} \\ \text{and} \\ \tfrac{f(u)}{u} \to \infty \text{ as } u \to \infty. \end{gathered} \tag{1.3}$$

We assume a smooth flux $f \in C^1$ and, without loss,

$$f(0) = f'(0) = 0. \tag{1.4}$$

The success of the nonlinear conservation law was highlighted for its shock wave theory, which was not possible with a local linear model. A convex flux or a genuinely nonlinear case is particularly well studied (see [6, 19, 20, 24]). However, the convex case is still in a stage between a local and the true global phenomenon, and one needs to study the nonconvex case to understand a real global phenomenon. The fluxes in Buckley-Leverett equation [26] and thin film equations [2] are good examples of nonconvex fluxes. The study of a nonconvex flux also has a long history (see [1, 7, 27]). In particular, asymptotics, regularity and solution structure are well studied for a single inflection point case (see more examples in [4, 5, 25]). However, the understanding of the nonconvex case is still far less than of a convex case because of its complexity. We suggest in this paper that a comprehensive survey for a fundamental solution will provide a better understanding of a nonconvex flux.

The construction of the fundamental solution with a nonconvex flux is obtained throughout this paper. The final formula of the fundamental solution is (4.9). Unfortunately, there is no simple and explicit formula for the nonconvex case. The solution is understood with the usual entropy condition or, equivalently, in the sense of Kružkov [19]. The construction of the fundamental solution is based on the dynamics of the convex-concave envelope, which gives similarity profiles that consist of a series of rarefaction waves and discontinuities. Even though the focus of this paper is construction itself, the detail of the structure can be obtained from the dynamics of the convex-concave envelope (see [17]).

The fundamental solution is the key in the theoretical development of a Cauchy problem. For an autonomous linear problem the solution is given by the convolution between the fundamental solution and the initial value. Even for nonlinear problems, the fundamental solution provides key information about the solution. The Oleinik inequality for a conservation law and the Aronson-Benilan inequality for a porous medium equation are basically comparisons of a solution to the fundamental solution. However, these inequalities fail for nonconvex flux or nonhomogeneous diffusion laws, and hence there have been

efforts to obtain such inequalities for general cases (see [9, 11, 12, 21]). Understanding the fundamental solution should be the first thing to do to extend the theory, and, in fact, such inequalities have been *unified* for a general class of PDEs by comparing a solution to the fundamental solution (see [16]). The asymptotics of an evolutionary problem in L^1 is a study of a process of how a solution turns into the shape of a fundamental solution (see, e.g., [3, 8, 14, 15, 18]). This is because the fundamental solution reflects the intrinsic properties.

The rest of the paper is as follows. In Section 2 we briefly give preliminaries about admissible weak solutions and explicit fundamental solutions in the convex case. In Section 3 the dynamics of the convex-concave envelope of a nonconvex flux is studied using the maximum of the fundamental solution as a parameter. We construct a fundamental solution in Section 4 using the convex-concave envelope and show that the constructed solution really is the admissible weak solution. Some of the basic structures are also introduced.

Scalar conservation laws have been used as test cases in the development of numerical schemes for hyperbolic problems. WENO, ENO and central schemes are some of them (see [10, 13, 23]). It is natural to ask if these schemes give the fundamental solution correctly even if there are several inflection points and the convex-concave envelope evolves drastically. In Section 5 the fundamental solutions are computed numerically using these schemes, where the numerical simulations show the evolution of the analytical fundamental solution correctly.

2. Preliminaries. The solution of (1.1) is defined in a weak sense that satisfies

$$\int\int (u\phi_t + f(u)\phi_x)dxdt + \int u^0(x)\phi(x,0)dx = 0 \tag{2.1}$$

for any test function $\phi \in C_0^\infty(\boldsymbol{R} \times [0,\infty))$. If a weak solution has a discontinuity along a curve $x = x(t)$, then it satisfies the Rankine-Hugoniot jump condition,

$$x'(t) = \frac{f(u_+(t)) - f(u_-(t))}{u_+(t) - u_-(t)}, \qquad u_\pm(t) = \lim_{y \to x(t)\pm} u(y,t). \tag{2.2}$$

A weak solution $u(x,t)$ is called the entropy solution if

$$\begin{cases} \ell(u) \le f(u) & \text{if } u_- \le u_+ \\ \ell(u) \ge f(u) & \text{if } u_- \ge u_+ \end{cases} \tag{2.3}$$

for all u between u_- and u_+, where $\ell(u)$ is the linear function connecting two states $(u_+, f(u_+))$ and $(u_-, f(u_-))$, i.e.,

$$\ell(u) = \frac{f(u_-) - f(u_+)}{u_- - u_+}(u - u_-) + f(u_-). \tag{2.4}$$

(One may read from this entropy condition that an increasing discontinuity should be given by the lower convex envelope since $\ell(u) \le f(u)$. Similarly, a decreasing one should be given by the upper concave envelope since $\ell(u) \ge f(u)$.) This entropy solution exists and is unique for a bounded measurable initial value, and this is the solution we consider. Readers are referred to Ballou [1] and Oleinik [24] for the well-posedness of the entropy

solution. For the unbounded initial value of the Dirac mass, the sign-changing solutions are not unique in general. However, our focus in this paper is a nonnegative solution, and the uniqueness of a signed solution is given by Liu and Pierre [22].

In summary, a piecewise smooth function is the entropy solution if it satisfies the equation (1.1) in smooth regions, every discontinuity satisfies the entropy condition (2.3), and discontinuity curves satisfy the Rankine-Hugoniot jump condition (2.2).

The structure of the conservation law (1.1) gives a similarity variable,

$$\xi = \frac{x}{t}.$$

A self-similar solution is a special one given in this similarity variable. The fundamental solution $\rho_m(x,t)$ will turn out to be a piecewise self-similar solution. Let a piecewise smooth solution be self-similar in a region and given by $u(x,t) = g(x/t)$. Then,

$$u_t + f'(u)u_x = -\frac{x}{t^2}g' + \frac{1}{t}f'(g)g' = 0,$$

and hence

$$f'\Big(g\Big(\frac{x}{t}\Big)\Big) = \frac{x}{t} \text{ or } f'(g(x)) = x. \tag{2.5}$$

The profile g that satisfies this relation is called a similarity profile. This relation gives a significant consequence that the similarity profile g should be an increasing function if f' is an increasing one. Hence, if the flux f is convex, then the decreasing part of a piecewise similarity solution should be a discontinuity that satisfies the Rankine-Hugoniot jump condition (2.2) and the entropy admissibility condition (2.3). If the flux is concave, then the similarity profile g is a decreasing function and the increasing part should be a discontinuity.

If the flux is strictly convex, $f''(u) > 0$, the fundamental solution $\rho_m(x,t)$ is given explicitly. Then, f' is invertible and the similarity profile $g(x)$ is given by

$$g = (f')^{-1} \text{ or } f'(g(x)) = x, \quad x \in \boldsymbol{R}. \tag{2.6}$$

The signed fundamental solution of mass $m > 0$ is explicitly given by

$$\rho_m(x,t) = \begin{cases} g(x/t), & 0 < x < \zeta_m(t), \\ 0\ , & \text{otherwise}, \end{cases} \tag{2.7}$$

where $\zeta_m(t) \geq 0$ is decided by the total mass relation

$$m = \int_0^{\zeta_m(t)} g(y/t)dy\,. \tag{2.8}$$

One may easily check that the fundamental solution satisfies

$$\rho_m(mx, mt) = \rho_1(x,t), \quad x \in \boldsymbol{R},\ t > 0. \tag{2.9}$$

Therefore, a single fundamental solution may cover all others.

For the Burgers equation case $f(u) = u^2/2$, the similarity profile becomes $g(x) = x$. Then, one can easily solve (2.8) and obtain

$$\zeta_m(t) = \sqrt{2mt},\ \rho_m(\zeta_m(t)-,t) = g(\zeta_m(t)/t) = \sqrt{2m/t}. \tag{2.10}$$

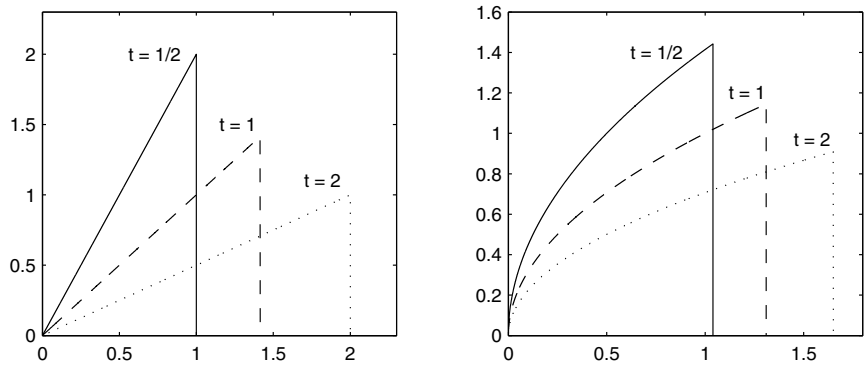

(a) fundamental solutions of Burgers (b) fundamental solutions of cubic law

FIG. 1. Graphs of a fundamental solution $\rho_1(x,t)$ are given at three instances: $t = 0.5, 1$ and 2. The Burgers case is with a flux $f(u) = u^2/2$, and the cubic law case is with $f(u) = u^3/3$.

In Figure 1(a), graphs of fundamental solutions with $m = 1$ is given at three instances: $t = 0.5, 1$ and 2. If the flux is given by a cubic law $f(u) = u^3/3$, then the similarity profile is $g(x) = \sqrt{x}$. In Figure 1(b), similar graphs are given at the same instances.

In summary, the fundamental solution of the conservation law has a simple structure if the flux is convex. Under the normalization assumption (1.4), the support of the fundamental solution is $[0, \zeta_m(t)]$ for some $\zeta_m(t) > 0$. The fundamental solution increases in the interval from $u = 0$ to the maximum value, say $u = \bar{u}$, and then drops to $u = 0$ at $x = \zeta_m(t)$ with an admissible discontinuity.

REMARK 2.1. The similarity profile g is actually a rarefaction wave for the convex flux case. However, we will see later that a similarity profile may include rarefaction waves, contact discontinuities and a shock for a nonconvex flux case. Furthermore, the profile is dynamically changing if the solution range is changed.

3. Convex and concave envelopes. If the flux f is not convex nor concave, then the relation (2.5) fails. In the next section we will see that the fundamental solution is constructed dynamically using convex-concave envelopes of the flux, but not directly by the flux. In this section we will first study the dynamics of convex-concave envelopes.

3.1. *Convex envelope.* The first step to construct a fundamental solution is to find the lower convex envelope of the given flux. The convex envelope on a given interval (u_1, u_2) is defined by

$$h(u; u_1, u_2) := \sup_{\eta \in A} \eta(u), \tag{3.1}$$

where

$$A := \{\eta \in C^2(\boldsymbol{R}) : \eta''(u) \geq 0,\ \eta(u) \leq f(u) \text{ for } u_1 < u < u_2\}. \tag{3.2}$$

Since there are only a finite number of inflection points, the convex envelope $h(u; u_1, u_2)$ is obtained by simply connecting the humps of the graph of the flux and the end points

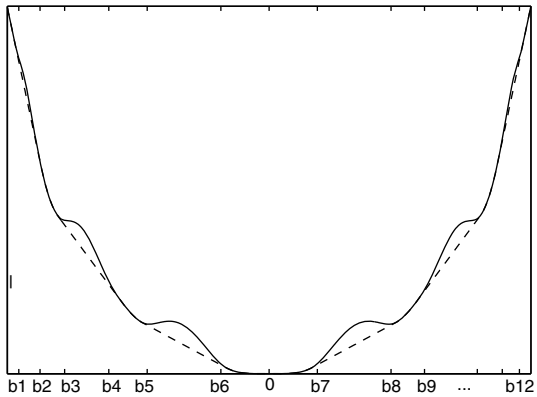

FIG. 2. A nonconvex flux $f(u)$ is given in a solid curve and its convex envelope $h(u)$ is in a dashed one, which is linear on intervals (b_{2i-1}, b_{2i}) and $h(u) = f(u)$ on the intervals (b_{2i}, b_{2i+1}).

$u = u_1$ and $u = u_2$ with tangent lines from below the graph (see Figure 2). For the case with the whole domain, we simply write it as $h(u)$.

The convex envelope $h(u)$ is a continuously differentiable function which is piecewise identical to $f(u)$ or piecewise linear. In other words, there exist strictly increasing sequences b_i, c_i, $i = 1, 2, \cdots, n$, such that

$$h'(u) = \begin{cases} c_i \quad , & b_{2i-1} < u < b_{2i}, \\ f'(u), & \text{otherwise.} \end{cases} \tag{3.3}$$

Consider a pseudo similarity profile $\tilde{g}(x)$ given by

$$\tilde{g}(0) = 0, \qquad h'(\tilde{g}(x)) = x, \qquad x \in \boldsymbol{R}, \tag{3.4}$$

which is piecewise continuous with discontinuities such that

$$\lim_{x \to c_i -} \tilde{g}(x) = b_{2i-1}, \quad \lim_{x \to c_i +} \tilde{g}(x) = b_{2i}$$

(see Figures 3(a) and 3(b)). Since h is a convex envelope, we have

$$f'(\lim_{x \to c_i -} \tilde{g}(x)) = h'(b_{2i-1}) = c_i = h'(b_{2i}) = f'(\lim_{x \to c_i +} \tilde{g}(x)). \tag{3.5}$$

Hence, this is a special kind of contact discontinuity, but not a genuine shock. In other words the pseudo similarity profile $\tilde{g}(x)$ consists of rarefaction waves and contact discontinuities.

Now we mimic the convex flux case to construct a pseudo fundamental solution with a nonconvex flux. Define a function by

$$\tilde{\rho}_m(x,t) = \begin{cases} \tilde{g}(x/t) \quad , & 0 < x < \tilde{\zeta}_m(t), \\ 0 \quad , & \text{otherwise,} \end{cases} \tag{3.6}$$

where $\tilde{\zeta}_m(t) \geq 0$ satisfies

$$m = \int_0^{\tilde{\zeta}_m(t)} \tilde{g}(y/t) dy \tag{3.7}$$

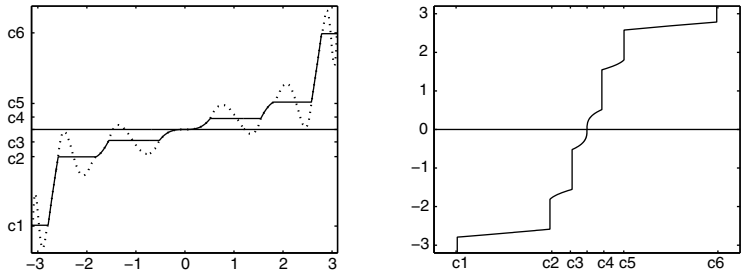

(a) $h'(u)$ is in line and $f'(u)$ in dots (b) Similarity profile $g = (h')^{-1}$

FIG. 3. (a) Graphs of $f'(u)$ and $h'(u)$ for the flux in Figure 2. (b) Similarity profile $g(x)$ consists of a series of rarefaction waves and discontinuities.

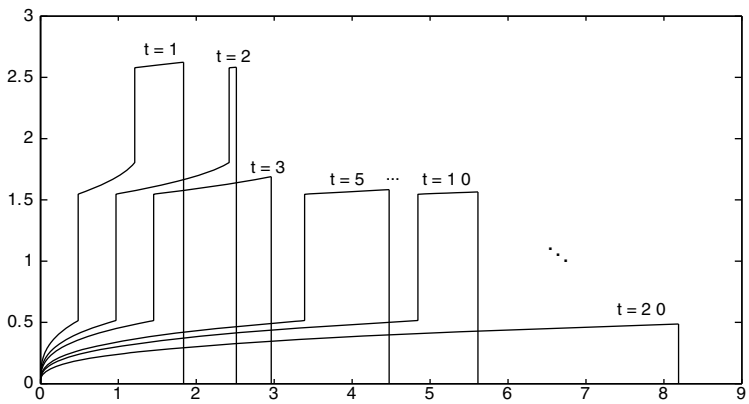

FIG. 4. Graphs of pseudo fundamental solution $\tilde{\rho}_m$ in (3.6) with $m = 3$ are given at several instances: $t = 1, 2, 3, 5, 10$ and 20. However, the shocks may violate the entropy condition.

(see Figure 4). One can easily check that this function satisfies the equation in (1.1) in smooth regions and the condition (1.2). At the increasing jumps the entropy condition (2.3) is satisfied since h is the convex envelope of f. The Rankine-Hugoniot jump condition is also satisfied. However, since f is not a convex function, there may exist $\bar{u} > 0$ such that the decreasing discontinuity from $u_- = \bar{u}$ and $u_+ = 0$ fails the entropy condition (2.3). Then, at the moment that $\tilde{\rho}_m(x,t)$ has such a value $\bar{u}$ as its maximum for the first time, it fails to be an admissible solution. In conclusion, we need to construct the correct decreasing profile which will be obtained from the concave envelope.

REMARK 3.1. It is natural to ask when $\tilde{\rho}_m(x,t)$ in (3.6) becomes a fundamental solution. One can easily see that if the graph of $f(u)$ is star-shaped with respect to the origin, the discontinuity at $x = \tilde{\zeta}_m(t)$ is admissible and hence it is a solution. Therefore, the convex flux f is a special case that makes $\tilde{\rho}_m(x,t)$ a fundamental solution. Even if f is not convex, under the hypothesis (1.3), there exists $u_0 > 0$ large such that the decreasing discontinuity that connects $u_- = \bar{u}$ and $u_+ = 0$ is admissible for all $\bar{u} > u_0$. Then, $\tilde{\rho}_m(x,t)$ is identical to the fundamental solution until $\max_x \tilde{\rho}_m(x,t) > u_0$. We will use

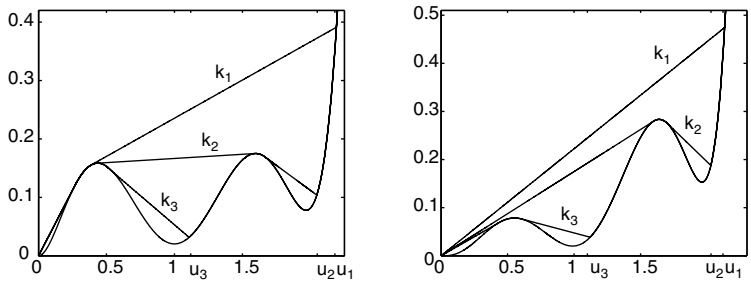

(a) Concave envelopes of $f_2(u)$ in (5.1) (b) Concave envelopes of $f_3(u)$ in (5.1)

FIG. 5. Concave envelopes $k_i := k(u; 0, u_i)$ give decreasing profile of a fundamental solution. A linear part indicates that there is a contact discontinuity connecting two end values. A part with $k(u; 0, u_i) = f(u)$ shows a rarefaction wave part that connects two contact discontinuities.

this fact later to choose an initial configuration for the construction of the fundamental solution.

3.2. *Concave envelope.* The next step is to find the upper concave envelope of the flux. The concave envelope on a given interval (u_1, u_2) is defined by

$$k(u; u_1, u_2) := \inf_{\eta \in B} \eta(u), \tag{3.8}$$

where

$$B := \{\eta \in C^2(\boldsymbol{R}) : \eta''(u) \le 0,\ \eta(u) \ge f(u) \text{ for } u_1 < u < u_2\}. \tag{3.9}$$

The concave envelope $k(u; u_1, u_2)$ is similarly obtained by connecting the humps of the graph of $y = f(u)$ and the end points from the above with tangent lines (see Figure 5). The concave envelope is the dual concept of the convex one and decides the shape of the decreasing side of a fundamental solution. The assumption that breaks a complete duality in this paper is the second hypothesis in (1.3), which assumes the convexity of f for u large.

REMARK 3.2. Consider a Riemann problem with an initial value

$$u^0(x) = \begin{cases} u_-, & x < 0, \\ u_+, & x > 0. \end{cases}$$

Then, the solution $u(x, t)$ is simply given by relations

$$\begin{aligned} th'(u(x,t); u_-, u_+) &= x, \quad \text{if } u_- < u_+, \\ tk'(u(x,t); u_+, u_-) &= x, \quad \text{if } u_- > u_+ \end{aligned}$$

(see [27]). Since the maximum and the minimum values are fixed, the convex and concave envelopes are also fixed. This makes the above formula work. However, for the fundamental solution case, the maximum decreases to zero and hence the convex-concave envelopes constantly evolve in time. To count such a change the left hand side of the above formula should be understood as an integral in time variable. The correct relations to construct the fundamental solution are given in (4.3) and (4.7).

In the following two lemmas we consider several obvious relations for concave and convex envelopes. These lemmas are useful in the following proofs and in finding the structure of a fundamental solution.

LEMMA 3.3. The convex and concave envelopes are ordered as

$$h(u; u_1, u_2) \le k(u; u_3, u_4), \quad u \in (u_1, u_2) \cap (u_3, u_4). \tag{3.10}$$

If $(u_1, u_2) \subset (u_3, u_4)$, then

$$k(u; u_1, u_2) \le k(u; u_3, u_4), \quad u \in (u_1, u_2), \tag{3.11}$$

$$h(u; u_1, u_2) \ge h(u; u_3, u_4), \quad u \in (u_1, u_2). \tag{3.12}$$

Proof. The relation (3.10) is clear since $h(u; a, b) \le f(u) \le k(u; a, b)$ for all $a < b$. Let $(u_1, u_2) \subset (u_3, u_4)$. Then, since the sets given in (3.9) are ordered as $B(u_3, u_4) \subset B(u_1, u_2)$, the corresponding infimums should be ordered as in (3.11). Similarly we have (3.12). □

The next lemma is for envelopes with $u_1 = 0$.

LEMMA 3.4. (*i*) If the convex envelope $h(u; 0, \bar{u}_0)$ is linear on $(a, b) \subset (0, \bar{u}_0)$, then $h(u; 0, \bar{u})$ is linear on (a, b) for all $\bar{u} \ge \bar{u}_0$. This property holds for the concave envelope, too.

(*ii*) At least one of $h(u; 0, \bar{u})$ and $k(u; 0, \bar{u})$ is linear on $(\bar{u} - \varepsilon, \bar{u})$ for an $\varepsilon > 0$ small.

Proof. (*i*) Suppose that $h(u; 0, \bar{u})$ is not linear on (a, b) for some $\bar{u} \ge \bar{u}_0$. Then there exists a subinterval $(c, d) \subset (a, b)$ on which $h(u; 0, \bar{u})$ is strictly convex and hence $h(u; 0, \bar{u}) = f(u)$. Since $h(u; 0, \bar{u}_0)$ is linear on (c, d) and is a lower convex envelope of $f(u)$, $h(u; 0, \bar{u}_0) < f(u) = h(u; 0, \bar{u})$ on the interval (c, d) after taking a smaller interval if needed. This contradicts Lemma 3.3 (3.12). Similar arguments hold for concave envelope $k(u; 0, \bar{u})$.

(*ii*) If $h(u; 0, \bar{u})$ is not locally linear near $u = \bar{u}$, then $h(u; 0, \bar{u}) = f(u)$ and is strictly convex for $u \in (\bar{u} - \varepsilon, \bar{u})$. Therefore, the concave envelope cannot be identical to $f(u)$ on the interval. Hence it should be linear on it. □

4. Construction of a fundamental solution.

4.1. *Nonconvex flux.* In this section we construct a signed fundamental solution. The construction in this paper is an extension of the convex flux case. We will present it step by step comparing it with the convex case and the figures.

The construction is given as a time integration of derivatives of convex-concave envelopes as in (4.3) and (4.7). We first construct the initial configuration at $t_0 > 0$ small. Due to the second hypothesis of (1.3) there exists $\bar{u} > 0$ large enough such that a decreasing discontinuity from $u_- = u$ to $u_+ = 0$ is admissible for all $u \ge \bar{u}$. Therefore, we have $\rho_m(x, t) := \tilde{\rho}_m(x, t)$ until that moment. Hence, there exist $t_0 > 0$ and $\zeta_m(t_0)$ such that

$$\tilde{g}(\zeta_m(t_0)/t_0) = u_0 \ge \bar{u} \text{ and } m = \int_0^{\zeta_m(t_0)} \tilde{g}(y/t_0)dy\,, \tag{4.1}$$

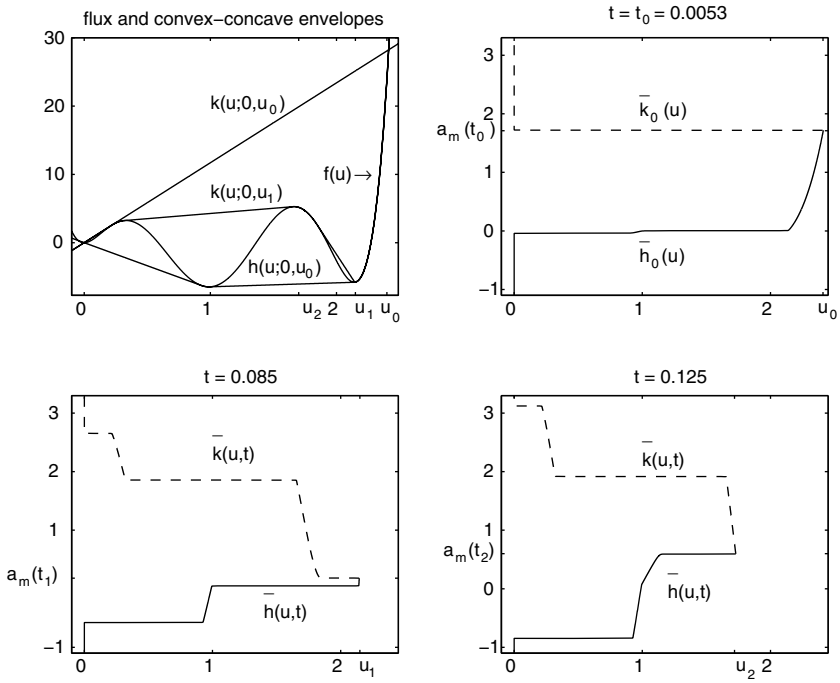

FIG. 6. The flux and the envelopes are given for two cases, $k_i := k(u;0,u_i)$, $h_i := h(u;0,u_i)$, $i = 0,1$. The value $u_0 > 0$ is taken large enough so that the shock connecting $u_- = u_0$ and $u_+ = u_0$ becomes admissible. This gives the initial profile $\bar{h}_0(u)$ and $\bar{k}_0(u)$. As $\bar{u}(t)$ decreases or as the time t increases, $\bar{h}(u,t)$ and $\bar{k}(u,t)$ may show interesting behavior.

where $\tilde{g}$ is the pseudo similarity profile given by (3.4). Let the boundary of the level set of the fundamental solution be

$$\bar{h}_0(u) = \inf\{x : \tilde{\rho}_m(x,t_0) > u\},\ \bar{k}_0(u) = \sup\{x : \tilde{\rho}_m(x,t_0) > u\}. \tag{4.2}$$

Gluing the graphs of $\bar{h}_0$ and $\bar{k}_0$ gives the graph of $\tilde{\rho}_m(x,t_0)$ of course. An example is given in Figure 6. In the top left figure, flux and convex-concave envelopes are given with a possible choice of $u_0 > 0$ that makes the concave envelope $k(u;0,u_0)$ a line. The corresponding time t_0 and the graphs of $\bar{h}_0$ and $\bar{k}_0$ are given in the top right figure, where the total mass is $m = 4$.

Consider the convex envelope $h(u;0,u_0)$ in the top left figure. Then there exists a maximal interval (v_0,u_0) such that $h(u;0,u_0) = f(u)$ on it and v_0 is a tangent point (v_0 is not marked in the figure). Notice that the concave envelope $k(u;0,\bar{u})$ changes drastically as $\bar{u}$ moves from u_0 to v_0. However, the convex envelope stays as it is except for a domain change. Therefore, for $v_0 < u < u_0$ and $t > t_0$, we define

$$\bar{h}(u,t) = \bar{h}_0(u) + \int_{t_0}^{t} h'(u;0,u_0)d\tau, \quad v_0 \le u \le u_0, \tag{4.3}$$

where the derivative in the integrand is with respect to u . One can easily see that $\bar{h}(u,t)$ is an increasing function with respect to the u variable since $h(u;0,u_0)$ is convex.

The next step is to find the maximum point $x = \zeta_m(t)$, which is the place that two profiles are glued. For the convex flux case this point is the right end point of the support, and hence it can be easily computed by the total mass relation (2.8). For a general nonconvex flux case it is still the maximum point, but it is not the end point of the support anymore. Hence we cannot use the total mass relation (2.8). The maximum point $x = \zeta_m(t)$ and the maximum value $\bar{u}(t)$ should be obtained by solving a system

$$a_m'(\tau) = \frac{f(\bar{u}(\tau)) - f(u_*(\tau))}{\bar{u}(\tau) - u_*(\tau)}, \tag{4.4}$$

$$\zeta_m(\tau) = \bar{h}(\bar{u}(\tau), \tau), \tag{4.5}$$

where the first equation is the Rankine-Hugoniot jump condition. The value $u_*(\tau)$ is an end of the linear part of the concave envelope $k(u; 0, \bar{u}(\tau))$ that connects this end to the maximum value $\bar{u}(\tau)$. Note that if $\bar{u}(\tau)$ is given, $u_*(\tau)$ can be explicitly computed. One can solve this system explicitly if the flux is convex, where such an example is given in Section 4.2. However, it is not possible for a general case, and so the fundamental solution is defined only implicitly.

Now we show that the maximum $\bar{u}(t)$ strictly decreases in time. Since the monotonicity is a local property, it is enough to consider $t_0 < t_1 < t_2$ with $|t_1 - t_2| \ll 1$ small enough. We consider the first stage for now so that $\bar{u}(t_2) > v_0$. By taking smaller $|t_1 - t_2|$ if needed we may assume, for all $t_1 < \tau < t_2$,

$$k'(\bar{u}(\tau); 0, \bar{u}(\tau)) < h'(\bar{u}(t_1); 0, u_0)$$

due to the relation between the convex and the concave envelopes or by Lemma 3.4(ii). Then, by (4.4) and (4.3), we have

$$\zeta_m'(\tau) = k'(\bar{u}(\tau); 0, \bar{u}(\tau)) < h'(\bar{u}(t_1); 0, u_0) = \partial_t \bar{h}(\bar{u}(t_1), \tau).$$

This strict inequality and (4.5) imply

$$\bar{h}(\bar{u}(t_2), t_2) = \zeta_m(t_2) < \bar{h}(\bar{u}(t_1), t_2).$$

Since $\bar{h}(\cdot, t)$ is a strictly increasing function in the region $u \in (v_0, u_0)$, we finally have a strict inequality,

$$\bar{u}(t_2) < \bar{u}(t_1) \text{ for all } t_1 < t_2. \tag{4.6}$$

Next, we define the decreasing side of the fundamental solution,

$$\bar{k}(u, t) = \bar{k}_0(u) + \int_{t_0}^{t} k'(u; 0, \bar{u}(\tau)) d\tau, \quad u < \bar{u}(t). \tag{4.7}$$

The concave envelope in the integrand changes drastically as the maximum $\bar{u}(\tau)$ moves from u_0 to v_0 (see the top left figure in Figure 6). One can easily check that since $k'(u; 0, \bar{u}(\tau)) = \frac{f(\bar{u}(\tau)) - f(u_*(\tau))}{\bar{u}(\tau) - u_*(\tau)}$ for any $v_0 < u < u_0$, $\bar{k}(u, t)$ actually moves with the same speed as $\zeta_m(t)$ and hence

$$\zeta_m(\tau) = \bar{k}(\bar{u}(\tau), \tau). \tag{4.8}$$

Therefore, $\bar{h}(\bar{u}(\tau),\tau) = \bar{k}(\bar{u}(\tau),\tau) = \zeta_m(\tau)$, and hence we may define the fundamental solution using the inverse relation of these functions:

$$\begin{cases} \bar{h}(\rho_m(x,t),t) & = x \text{ for } x < \zeta_m(t), \\ \bar{k}(\rho_m(x,t),t) & = x \text{ for } x > \zeta_m(t). \end{cases} \tag{4.9}$$

In the bottom left of Figure 6, graphs of $\bar{h}$ and $\bar{k}$ are displayed at $t = 0.085$ when $\bar{u}(t) = u_1$ is slightly bigger than the tangent point v_0. As $\bar{u}(t)$ approaches v_0 the thin spike in the figure becomes thinner and eventually disappears as in the bottom right of Figure 6. At the moment, the maximum jumps from $\bar{u}(t) = v_0$ to $u_*(t)$, which is the other end of the linear part of the concave envelope at the moment of collapse of the thin spike. The first stage of the fundamental solution is completed.

In the second stage, the roles of convex and concave envelopes are exchanged. Let (v_1, u_*) be the maximal interval such that $k(u;0,u_*) = f(u)$ on it. In the second stage the fundamental solution is constructed similarly in the interval $v_1 < u < u_*$. Since we have assumed that there are a finite number of inflection points, this process will be done in finite steps, and hence the construction of the fundamental solution is complete now.

REMARK 4.1. One can clearly see that $\bar{u}(t)$ which was employed in the construction is the maximum of the fundamental solution. The monotonicity in (4.6) now implies that maximum of the fundamental solution decreases strictly as $t \to \infty$.

REMARK 4.2. For a convex flux case the inverse relation of the flux is considered first to find the similarity profile g, and then the time effect is counted simply by $g(x/t)$ as in (2.7). However, for the nonconvex case, the convex-concave envelope changes as the maximum of the fundamental solution changes. Therefore, the time effect is considered first as in (4.3) and then the inverse relation (4.9) is taken.

The discontinuities of the fundamental solution constructed so far satisfy the entropy condition, since they are all from convex-concave envelopes, which produces admissible discontinuities only. These discontinuities also satisfy the Rankine-Hugoniot jump condition, since the discontinuity at the maximum point $\zeta_m(t)$ satisfies (4.4), which is actually from the jump condition. All the other discontinuities are of the contact type that satisfy (3.5). Hence, the constructed function $\rho_m(x,t)$ is really the fundamental solution satisfying the entropy condition if we show that $\rho_m(x,t)$ satisfies the conservation law in a classical sense in smooth regions.

Assume that $\rho_m(x,t)$ is smooth at (x,t) such that $x < \zeta_m(t)$. First differentiate the first relation in (4.9) with respect to x and t and obtain

$$\frac{\partial}{\partial x}\Big(\bar{h}(\rho_m(x,t),t)\Big) = \frac{\partial}{\partial u}\bar{h}\,\frac{\partial}{\partial x}\rho_m = 1, \tag{4.10}$$

$$\frac{\partial}{\partial t}\Big(\bar{h}(\rho_m(x,t),t)\Big) = \frac{\partial}{\partial u}\bar{h}\,\frac{\partial}{\partial t}\rho_m + \frac{\partial}{\partial t}\bar{h} = 0. \tag{4.11}$$

On a rarefaction wave part, the convex envelope and the flux itself are identical. Therefore, from (4.3),

$$\frac{\partial}{\partial t}\bar{h}(\rho_m(x,t),t) = h'(\rho_m(x,t);0,\bar{u}(t)) = f'(\rho_m(x,t)). \tag{4.12}$$

Substituting (4.10) and (4.12) into (4.11), we finally obtain

$$\frac{\partial}{\partial t}\rho_m(x,t) + f'(\rho_m(x,t))\frac{\partial}{\partial x}\rho_m(x,t) = 0.$$

On the region $x > \zeta_m(t)$, one can similarly show an equation by differentiating the second relation in (4.9), which completes the proof.

In summary, we conclude the construction of the fundamental solution in this section with a theorem.

THEOREM 4.3. Let the flux f satisfy (1.3). The function $\rho_m(x,t)$ given by the relation (4.9) is the nonnegative fundamental solution of (1.1) that satisfies the entropy condition. For any $t_1 < t_2$,

$$\max_x \rho_m(x,t_2) < \max_x \rho_m(x,t_1). \tag{4.13}$$

Now we discuss several basic properties of $\bar{h}$ and $\bar{k}$. These provide key structures of fundamental solutions (see [17] for detailed structure of fundamental solutions).

LEMMA 4.4. (*i*) $\bar{h}(u,t)$ and $\bar{k}(u,t)$ are continuous for all $t \geq t_0$.

(*ii*) If the convex envelope $h(u;0,\bar{u}(t))$ has a linear part that connects $u = a$ and $u = b$, then $\bar{h}(u,t)$ is constant for $u \in (a,b)$, and hence $\rho_m(x,t)$ has an increasing discontinuity that connects $u_- = a$ and $u_+ = b$. Similarly, a linear part of the concave envelope gives $\rho_m(x,t)$ a decreasing discontinuity.

(*iii*) The maximum point $(\zeta_m(t),\bar{u}(t))$ of a fundamental solution is always connected to a shock on one side and a rarefaction wave on the other.

Proof. (*i*) Since the envelopes are continuously differentiable, $\bar{h}(u,t)$ and $\bar{k}(u,t)$ are continuous.

(*ii*) Lemma 3.4 implies that $h'(u;0,\bar{u}(\tau))$ is constant for $u \in (a,b)$ for any given time $0 < \tau < t$. Therefore, its integral with respect to time variable (4.3) is also constant on the interval. From the construction of $\tilde{\rho}_m(x,t)$, $\bar{h}_0(u)$ is constant on the interval. Therefore, $\bar{h}(u,t)$ is constant on (a,b), and hence the inverse relation $\rho_m(x,t)$ has the discontinuity in the claim. Similar arguments hold for concave envelopes.

(*iii*) If the maximum point is connected to shocks on both sides, this means it has a removable jump at the point. Lemma 3.4(*ii*) implies that the maximum point cannot be connected by two rarefaction waves. Therefore, the maximum point is connected by an increasing shock and a decreasing rarefaction or an increasing rarefaction and a decreasing shock. □

4.2. *Examples and comparison with a convex case.* In this section we consider examples that show the structure of the fundamental solution $\rho_m(x,t)$ constructed in the previous section. First, we review the fundamental solution of the Burgers equation and compare it with a general nonconvex case in this paper. We will observe that the construction of the fundamental solution in this paper is a natural generalization of the well-known Burgers equation case.

The flux of the Burgers equation is $f(u) = u^2/2$, which is convex. Therefore, the convex envelope is simply $h(u;0,\bar{u}) = f(u)$, and the concave envelope is the linear line connecting the origin and $(\bar{u}, f(\bar{u}))$, i.e., $k(u;0,\bar{u}) = \frac{\bar{u}}{2}u$. For the initial time we may

take $t_0 = 1$. Then, one can easily compute that $h'(u; 0, \bar{u}(t)) = u, k'(u; 0, \bar{u}(t)) = \bar{u}(t)/2$, $\zeta_m(1) = \bar{u}(1) = \sqrt{2m}$, and hence the initial profiles in (4.2) are given by

$$\bar{h}_0(u) = u, \qquad \bar{k}_0(u) = \sqrt{2m}.$$

Therefore,

$$\bar{h}(u,t) = u + \int_1^t u dt = tu, \quad \bar{k}(u,t) = \sqrt{2m} + \int_1^t \bar{u}(t)/2 dt.$$

Now we solve $\zeta_m(t)$ and $\bar{u}(t)$ in (4.4)-(4.5). Since

$$\zeta_m(t_0 = 1) = \sqrt{2m}, \quad \zeta_m(t) = \bar{h}(\bar{u}(t), t) = t\bar{u}(t), \quad \frac{f(\bar{u}(t))}{\bar{u}(t)} = \frac{\bar{u}(t)}{2},$$

equation (4.4) becomes

$$\zeta_m'(t) = \zeta_m(t)/2t, \qquad \zeta_m(1) = \sqrt{2m}.$$

One may compute this first order equation and obtain

$$\zeta_m(t) = \sqrt{2mt}, \qquad \bar{u}(t) = \sqrt{2m/t},$$

which are identical to the values in (2.10).

For a general nonconvex flux case it is not possible to solve the equations by hand, and one needs to compute it numerically using the appropriate iterative method. However, the properties given in Lemmas 3.4 and 4.4 give us a chance to see the structure of the fundamental solution via the structures of $\bar{h}(u,t)$ and $\bar{k}(u,t)$.

In Figure 6 several examples are given. In the first figure the graph of the flux and convex-concave envelopes are shown. Since the convex envelope has a linear part with negative slope, the corresponding discontinuity has a negative speed. The concave envelope $k(u; 0, u_0)$ is a straight line. One can find in the figure at $t = 0.0053$ that $\bar{k}_0(u)$ is constant. The convex envelope $h(u; 0, u_0)$ consists of two linear parts and two tangent parts. In the graph of $\bar{h}_0(u)$ one can find two constant parts and two rarefaction parts.

The concave envelope $k(u; 0, u_1)$ consists of three straight lines and two curves tangent to $f(u)$. One can find from the figure at $t = 0.085$ that $\bar{k}(u,t)$ has three constant parts and two rarefaction (or nonconstant) waves. The convex envelope $h(u; 0, u_1)$ consists of two linear parts and one tangent part. In the graph of $\bar{h}(u,t)$ one can find two constant states and one rarefaction wave. Notice that at the right end of the thin peak, there is a tiny rarefaction wave. That means that u_1 is slightly bigger than the tangent point v_0 of the convex envelope.

If the maximum $\bar{u}(t)$ arrives at the tangent value v_0, then the thin peak will disappear and there will be a jump in the maximum from v_0 to u_*. This peak is gone in the figure at $t = 0.125$. One interesting point is the angle in the middle of the rarefaction wave of $\bar{h}(u,t)$ in the last picture. This is due to the sudden change of the convex envelope that happened when the peak collapsed. The corresponding fundamental solution is obtained from the relations in (4.9). Therefore, the fundamental solution is obtained by simply reflecting the figures with respect to the line $y = x$. As we have observed from these examples the dynamics of envelopes indicates the dynamics of the fundamental solution in detail.

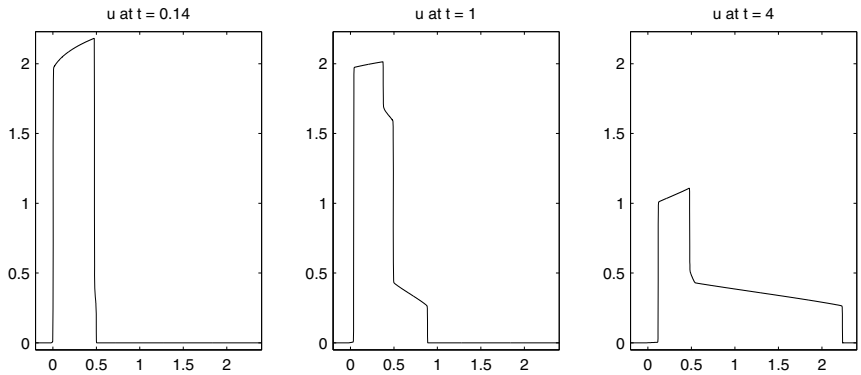

FIG. 7. Numerical computations for $\rho_1(x,t)$ are given at three instances. The flux is f_2 in (5.1) or in Figure 5(a). WENO is used for this numerical computation.

5. Numerical examples. The purpose of this section is to construct fundamental solutions numerically and compare them to the analytic ones constructed in the previous section. In these computations we have used WENO and a central type scheme. In many cases simplified numerical schemes are used under a convexity assumption. Hence one should modify such parts and use such schemes with their full complexity. We were curious if these numerical schemes solve the conservation law without convexity correctly. The numerical solutions in this section explain the structure of the fundamental solution discussed in the previous section, and hence one may be convinced that both the numerical schemes and the analysis are correct.

For the comparison we took nonconvex fluxes

$$f_n(u) = u^n(u^2 - 2u + 1.02)(u^2 - 4u + 4.02), \quad n \geq 2, \tag{5.1}$$

which satisfies the hypotheses (1.3) and (1.4). Furthermore, this flux satisfies

$$f(u) > 0 \quad \text{for} \quad u > 0, \tag{5.2}$$

which may make the situation simpler. Graphs of these fluxes are given in Figure 5. For a numerical computation one should consider an appropriate initial value. Since the Dirac-delta measure cannot be used directly, we took an initial value

$$u_0(x) = \begin{cases} m/\epsilon, & 0 < x < \epsilon, \\ 0, & \text{otherwise} \end{cases} \tag{5.3}$$

for m/ε large. In fact, if the jump from $u_- = m/\varepsilon$ to $u_+ = 0$ is admissible, one may show $u(x,t) = \rho_m(x,t)$ for all $t > t_0$ such that $\max u(x,t_0) < m/\epsilon$.

In Figure 7, intermediate states of the fundamental solution $\rho_1(x,t)$ are given at three instances. The first one, at $t = 0.14$, has the maximum value corresponding to u_1 in Figure 5(a). The concave envelope at the moment consists of two linear parts and one rarefaction part. Since the amount of time to form a rarefaction is short, one can barely find a rarefaction wave in the figure. One can find the corresponding rarefaction wave more clearly when $t = 1$. The concave envelope with the maximum u_2 in Figure 5(a) has

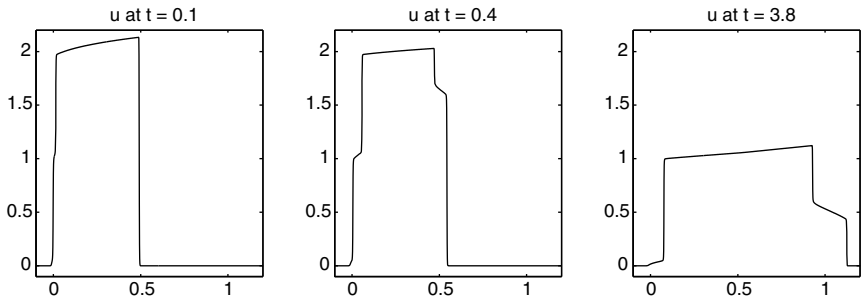

FIG. 8. Numerical computations for $\rho_1(x,t)$ are given at three instances. The flux is f_3 in (5.1) or in Figure 5(b). WENO is used for this numerical computation.

three linear and two rarefaction parts. One can find them in the decreasing profile of the fundamental solution at time $t = 1$. At a later time $t = 4$, the corresponding maximum is u_3, and the concave envelope has two linear parts and one rarefaction part. In the figure at $t = 4$ one can observe two shocks and one rarefaction wave after the maximum point.

In Figure 8 another example for intermediate states of a fundamental solution are given with the flux function f_3 in (5.1). The figures of its graph and concave envelopes are given in Figure 5(b). The first one at $t = 0.1$ has the maximum value corresponding to u_1. The concave envelope at the moment is a line. One can see a discontinuity that connects u_1 and 0. The second figure at $t = 0.4$ is the moment with the maximum u_2 and the concave envelope has two linear parts divided by a rarefaction wave. One can find them in the decreasing profile of the fundamental solution. At time $t = 3.8$, the corresponding maximum is u_3 and the concave envelope has two linear parts and one rarefaction wave. One can find two shocks and one rarefaction in the figure. In this discussion, we have only discussed the relation between the concave envelopes and the decreasing profile of the fundamental solution. Readers may compare the convex envelopes and the increasing profiles of these examples similarly.

Now we discuss the asymptotic structure. Notice that even if the formulas in (4.3) and (4.7) give us a view for the structure of fundamental solutions in detail, it is not easy to compute it exactly. That is why we could not display the examples in Figures 7 and 8 with exact solutions. However, for the asymptotic structure, one can explicitly compute a fundamental solution $\rho_m(x,t)$ for t large if

$$f(u) > 0, \qquad u \neq 0.$$

Then, if the maximum of the fundamental solution is less than the smallest tangent value of the convex envelope, then $\rho_m(x,t) = \tilde{\rho}_m(x,t)$, and hence one can explicitly compute the fundamental solution.

In Figure 9(a) the fundamental solution $\rho_{0.5}(x,t)$ is given in a solid line together with a numerical solution, where the flux is f_4 in (5.1). For an easier comparison with the exact solution the numerical solution is plotted using fewer grid points. One can clearly see that the numerical solution matches the exact solution. For this numerical example

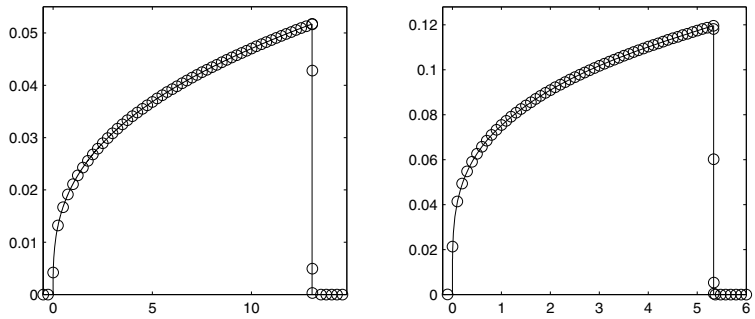

(a) Flux is (5.1) with $n = 4$ ($t = 7,000$) (b) Flux is (5.1) with $n = 5$ ($t = 2,000$)

FIG. 9. The fundamental solution $\rho_{0.5}(x,t)$ is in solid lines, and its numerical simulation is in dots. A central type scheme is used for the numerical solution.

we used the central scheme. The example with f_n with $n = 5$, Figure 9(b), also matches the exact one well.

References

[1] Donald P. Ballou, *Solutions to nonlinear hyperbolic Cauchy problems without convexity conditions*, Trans. Amer. Math. Soc. **152** (1970), 441–460 (1971). MR0435615 (55 #8573)

[2] A. L. Bertozzi, A. Münch, and M. Shearer, *Undercompressive shocks in thin film flows*, Phys. D **134** (1999), no. 4, 431–464, DOI 10.1016/S0167-2789(99)00134-7. MR1725916 (2001e:76042)

[3] José A. Carrillo and Juan L. Vázquez, *Fine asymptotics for fast diffusion equations*, Comm. Partial Differential Equations **28** (2003), no. 5-6, 1023–1056, DOI 10.1081/PDE-120021185. MR1986060 (2004a:35118)

[4] Kuo Shung Cheng, *Asymptotic behavior of solutions of a conservation law without convexity conditions*, J. Differential Equations **40** (1981), no. 3, 343–376, DOI 10.1016/0022-0396(81)90003-6. MR621249 (82h:35008)

[5] Kuo Shung Cheng, *A regularity theorem for a nonconvex scalar conservation law*, J. Differential Equations **61** (1986), no. 1, 79–127, DOI 10.1016/0022-0396(86)90126-9. MR818862 (88e:35121)

[6] C. M. Dafermos, *Generalized characteristics and the structure of solutions of hyperbolic conservation laws*, Indiana Univ. Math. J. **26** (1977), no. 6, 1097–1119. MR0457947 (56 #16151)

[7] C. M. Dafermos, *Regularity and large time behaviour of solutions of a conservation law without convexity*, Proc. Roy. Soc. Edinburgh Sect. A **99** (1985), no. 3-4, 201–239, DOI 10.1017/S0308210500014256. MR785530 (86j:35107)

[8] Jean Dolbeault and Miguel Escobedo, *L^1 and L^∞ intermediate asymptotics for scalar conservation laws*, Asymptot. Anal. **41** (2005), no. 3-4, 189–213. MR2127996 (2006i:35233)

[9] Olivier Glass, *An extension of Oleinik's inequality for general 1D scalar conservation laws*, J. Hyperbolic Differ. Equ. **5** (2008), no. 1, 113–165, DOI 10.1142/S0219891608001398. MR2405854 (2009c:35292)

[10] Youngsoo Ha and Yong Jung Kim, *Explicit solutions to a convection-reaction equation and defects of numerical schemes*, J. Comput. Phys. **220** (2006), no. 1, 511–531, DOI 10.1016/j.jcp.2006.07.018. MR2281641 (2007k:65119)

[11] David Hoff, *The sharp form of Oleĭnik's entropy condition in several space variables*, Trans. Amer. Math. Soc. **276** (1983), no. 2, 707–714, DOI 10.2307/1999078. MR688972 (84b:35080)

[12] Helge Kristian Jenssen and Carlo Sinestrari, *On the spreading of characteristics for nonconvex conservation laws*, Proc. Roy. Soc. Edinburgh Sect. A **131** (2001), no. 4, 909–925, DOI 10.1017/S0308210500001189. MR1855004 (2002h:35179)

[13] Guang-Shan Jiang and Chi-Wang Shu, *Efficient implementation of weighted ENO schemes*, J. Comput. Phys. **126** (1996), no. 1, 202–228, DOI 10.1006/jcph.1996.0130. MR1391627 (97e:65081)

[14] Yong Jung Kim, *Asymptotic behavior of solutions to scalar conservation laws and optimal convergence orders to N-waves*, J. Differential Equations **192** (2003), no. 1, 202–224, DOI 10.1016/S0022-0396(03)00058-5. MR1987091 (2004e:35147)

[15] Yong-Jung Kim, *Potential comparison and asymptotics in scalar conservation laws without convexity*, J. Differential Equations **244** (2008), no. 1, 40–51, DOI 10.1016/j.jde.2006.08.013. MR2373653 (2009d:35220)

[16] Yong-Jung Kim, *A geometric one-sided inequality for zero-viscosity limits*, preprint, http://amath.kaist.ac.kr/papers/Kim/32.pdf (2014).

[17] Yong-Jung Kim and Young-Ran Lee, *Structure of the fundamental solution of a nonconvex conservation law*, to appear in Proc. Roy. Soc. Edinburgh Sect. A–Math., http://amath.kaist.ac.kr/papers/Kim/17.pdf.

[18] Yong Jung Kim and Robert J. McCann, *Potential theory and optimal convergence rates in fast nonlinear diffusion* (English, with English and French summaries), J. Math. Pures Appl. (9) **86** (2006), no. 1, 42–67, DOI 10.1016/j.matpur.2006.01.002. MR2246356 (2007f:35163)

[19] S. N. Kružkov, *First order quasilinear equations with several independent variables* (Russian), Mat. Sb. (N.S.) **81 (123)** (1970), 228–255. MR0267257 (42 #2159)

[20] P. D. Lax, *Hyperbolic systems of conservation laws. II*, Comm. Pure Appl. Math. **10** (1957), 537–566. MR0093653 (20 #176)

[21] Philippe G. Lefloch and Konstantina Trivisa, *Continuous Glimm-type functionals and spreading of rarefaction waves*, Commun. Math. Sci. **2** (2004), no. 2, 213–236. MR2119939 (2005i:35174)

[22] Tai-Ping Liu and Michel Pierre, *Source-solutions and asymptotic behavior in conservation laws*, J. Differential Equations **51** (1984), no. 3, 419–441, DOI 10.1016/0022-0396(84)90096-2. MR735207 (85i:35094)

[23] Haim Nessyahu and Eitan Tadmor, *Nonoscillatory central differencing for hyperbolic conservation laws*, J. Comput. Phys. **87** (1990), no. 2, 408–463, DOI 10.1016/0021-9991(90)90260-8. MR1047564 (91i:65157)

[24] O. A. Oleĭnik, *Discontinuous solutions of non-linear differential equations* (Russian), Uspehi Mat. Nauk (N.S.) **12** (1957), no. 3(75), 3–73. MR0094541 (20 #1055)

[25] Tao Tang, Zhen-Huan Teng, and Zhouping Xin, *Fractional rate of convergence for viscous approximation to nonconvex conservation laws*, SIAM J. Math. Anal. **35** (2003), no. 1, 98–122, DOI 10.1137/S0036141001388993. MR2001466 (2004i:35221)

[26] C. J. van Duijn, L. A. Peletier, and I. S. Pop, *A new class of entropy solutions of the Buckley-Leverett equation*, SIAM J. Math. Anal. **39** (2007), no. 2, 507–536 (electronic), DOI 10.1137/05064518X. MR2338418 (2008g:35136)

[27] Burton Wendroff, *The Riemann problem for materials with nonconvex equations of state. I. Isentropic flow*, J. Math. Anal. Appl. **38** (1972), 454–466. MR0328387 (48 #6729)